

Spring 4-16-2019

Nanomedical Applications in Zebrafish: Characterizing VLP HK97 as a Cell-Specific Delivery Tool in Danio Rerio

Bridget A. Fitzgerald
University of Texas at Tyler

Follow this and additional works at: https://scholarworks.uttyler.edu/biology_grad



Recommended Citation

Fitzgerald, Bridget A., "Nanomedical Applications in Zebrafish: Characterizing VLP HK97 as a Cell-Specific Delivery Tool in Danio Rerio" (2019). *Biology Theses*. Paper 57.
<http://hdl.handle.net/10950/1306>

This Thesis is brought to you for free and open access by the Biology at Scholar Works at UT Tyler. It has been accepted for inclusion in Biology Theses by an authorized administrator of Scholar Works at UT Tyler. For more information, please contact tgullings@uttyler.edu.

NANOMEDICAL APPLICATIONS IN ZEBRAFISH:
CHARACTERIZING VLP HK97 AS A CELL-SPECIFIC DELIVERY
TOOL IN DANIO RERIO

by

BRIDGET A. FITZGERALD

A thesis submitted in partial fulfillment of
the requirements for the degree of
Master of Science
Department of Biology

Brent R. Bill, Ph.D., Committee Chair
College of Arts and Sciences

University of Texas at Tyler
May 2019

The University of Texas at Tyler
Tyler, TX

This is to certify that the master's Thesis of

BRIDGET A. FITZGERALD

Has been approved for the thesis requirements on

March 20th, 2019

For the Master of Science in Biology degree

Approvals:



Thesis Chair: Dr. Brent R. Bill, Ph.D.



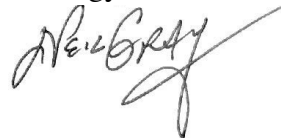
Committee Member: Dr. Ali Azghani, Ph.D.



Committee Member: Dr. Dustin Patterson, Ph.D.



Chair, Department of Biology: Dr. Lance Williams Ph.D.



Dean, College of Arts and Sciences

Acknowledgements

I would like to thank my family and friends, specifically my parents Dr. Kathleen A. Fitzgerald and Patrick J. Fitzgerald for their unwavering love and support throughout this process.

Thank you to my committee members Dr. Ali Azghani and Dr. Dustin Patterson for their guidance throughout my time at UT Tyler.

I would like to thank Dr. Dustin Patterson for his expertise and guidance throughout the entirety of my project. I would also like to thank Dr. Patterson and his lab including undergraduate researcher Michael J. King for synthesizing the VLPs used in this project.

I would like to thank Dr. Eleanor Chen for the Rag2:KRAS and Rag2:DSRED plasmids. Thank you to undergraduate researcher Baylie S. Catrett for her work in data analysis and undergraduate researcher Olivia G. Brandenburg for her work on the toxicity profile.

I would like to thank the Texas Academy of Science for their partial funding of this project.

Finally, I would like to thank Dr. Brent Bill and Mrs. Ashley Bill. Without their support both inside and outside of the lab none of my success would have been possible.

Table of Contents

List of Tables.....	iv
List of Figures.....	v
Abstract.....	vi
Chapter 1: Introduction.....	1
Site Selectivity of Pharmaceuticals.....	1
Virus Like Particles (VLPs)	1
Nanomedicine.....	3
VLP HK97.....	6
Zebrafish: A Complementary System for Nanomedical Applications of VLP HK97.....	7
Ideal Disease Models for VLP HK97: Rhabdomyosarcoma.....	8
VLP Design Strategy.....	10
Chapter 2: Materials and Methods.....	13
Zebrafish Housing & Husbandry.....	13
Synthesis of VLP HK97.....	13
Synthesis of <i>rag2:DSRED</i> & <i>rag2:kRAS12D</i>	14
Embryo Collection & Injection.....	15
Toxicity Profile.....	15
Viability Screening.....	15
Morphological Toxicity.....	15
Physiological Toxicity.....	16
Neural Toxicity.....	16

VLP Localization.....	17
Embryonic Localization.....	17
Larval Localization.....	17
Adult Localization.....	17
Data Analysis.....	18
Chapter 3: Results.....	19
Toxicity Profile.....	19
Viability Screening.....	19
Morphological Toxicity.....	21
Physiological Toxicity.....	25
Neural Toxicity.....	25
VLP HK97 Localization.....	26
Embryonic Localization.....	26
Larval Localization.....	28
Adult Localization.....	30
zRMS tumorigenesis.....	30
Chapter 4: Discussion.....	32
Toxicity Profile.....	32
Unmodified VLP HK97.....	32
VLP HK97:FITC:RGD.....	33
VLP HK97 Localization.....	34
Embryonic Localization.....	34
Larval Localization.....	35

Adult Localization.....	36
Rhabdomyosarcoma Model in Zebrafish.....	36
References.....	38

List of Tables

Table 1. Summary of the toxicity profile.....	26
--	----

List of Figures

Figure 1. Design strategy for cell-specific targeting and localization of VLP HK97.....	12
Figure 2. Plasmid maps.....	14
Figure 3. Sectioning schema for adult zebrafish treated with VLP HK97.....	18
Figure 4. Viability of embryos at 1dpf following injection of unmodified VLP HK97.....	19
Figure 5. Viability measures after the addition of the RGD cell targeting peptide.....	20
Figure 6. Developmental delay measured by assessing morphological age.....	21
Figure 7. Tail deformities are observed at the highest injection dose.....	22
Figure 8. Pericardial cell death is observed at high injection observed at 2dpf after injection.....	23
Figure 9. Alcian blue stain reveals no deformities of major cartilaginous structures in zebrafish at 5dpf.....	24
Figure 10. Unmodified VLP HK97 shows no toxic effects on heart rate.....	25
Figure 11. Injection of single cell embryos with FITC labeled VLP HK97.....	26
Figure 12. The addition of the RGD cell targeting peptide results in non-uniform entrance.....	27
Figure 13. Percentage of embryos which exhibit non-uniform distribution.....	28
Figure 14. VLP HK97:FITC:RGD localizes to known regions of integrin expression.....	29
Figure 15. VLP HK97:FITC:RGD localizes to known regions of integrin expression.....	29
Figure 16. VLP HK97 does not localize to specific body regions.....	30
Figure 17. Successful induction of tumorigenesis in zebrafish.....	30

Abstract

NANOMEDICAL APPLICATIONS IN ZEBRAFISH: CHARACTERIZING VLP HK97 AS A CELL-SPECIFIC DELIVERY TOOL IN DANIO RERIO

Bridget A. Fitzgerald

Thesis Chair: Dr. Brent Bill

The University of Texas at Tyler
May 2019

Virus Like Particles (VLPs) are self-assembling protein subunits which organize *in vitro* into hollow protein cages that mimic the structure of a viral capsid. VLPs possess valuable characteristics of the native virus including immunogenicity and a propensity for entrance into cells. However, they lack the viral genome and the ability to replicate, rendering them non-virulent. VLPs can be internally and externally modified utilizing genetic engineering and biochemical techniques. Applications of modified VLPs are vast in nanomedicine, and tissue-specific drug targeting is a desirable potential use for this technology. VLP HK97 is a well characterized VLP derived from a bacteriophage found in *E.coli* and has yet to be tested in the zebrafish model. Experiments show unmodified VLP HK97 is non-toxic at biologically relevant doses in zebrafish, making this particle a viable option for further study with the addition of cell penetrating peptides (CPPs). The addition of RGD onto the external surface of VLP HK97, a cell targeting peptide known to target integrin receptors, drastically decreased the amount of VLP tolerated by the zebrafish. Further localization experiments reveal that this may be due to increased localization into distinct cell subtypes in the zebrafish embryo. The modified particle also showed localization to known sites of integrin expression in larval zebrafish. These

experiments conclude that VLP HK97 is a viable candidate as a drug delivery platform.

VLP HK97 is a viable platform for testing cell-specific targeting for drugs and other molecules in a wide variety of zebrafish disease models.

Chapter 1

Introduction

Site Selectivity in Pharmaceuticals

Selectivity refers to the degree to which a drug can reach its target site relative to other sites within the body¹. Current efforts aim to design drugs with high site selectivity as this increases the drug's ability to enact change on the target tissue and also reduces harmful side effects caused by the drug. As site selectivity increases, a drug's efficacy increases¹. Lack of site selectivity is a prevalent issue within medical and pharmaceutical industries which leads to the persistence of disease and the prevalence of unwanted side effects for many patients.

Detrimental issues due to a lack of site specificity is most obvious in the collection of cancer drugs currently used for treatment. Current chemotherapeutics and radiation therapies function by damaging nuclear DNA and initiating apoptosis^{2,3}. This occurs more quickly in the faster dividing cancerous cells; however, healthy cells are also damaged as a result of using these. Lack of site selectivity in these treatments causes healthy cells to die leading to vast unsatisfactory side effects affecting every organ system in the body⁴. Current drug development aims to optimize site selectivity, providing more efficacious drugs and minimizing off target effects. Virus Like Particles (VLPs) provide a versatile platform for increasing site selectivity for a variety of pharmaceuticals.

Virus-Like Particles (VLPs)

Virus-like particles (VLPs) are comprised of small protein subunits derived from native viruses which are capable of assembling *in vitro* into hollow protein cages which mimic the structure of a viral capsid⁵. These proteins can be derived from a multitude of host sources

including bacteria, yeast, and mammalian cell host systems with over 110 VLPs being constructed from these systems as of 2013⁶⁻⁸. These particles possess valuable characteristics of the native viruses including immunogenic properties and a propensity for entrance into cells^{5,9}. Properties include heightened B cell activation, cellular and humoral immune response, and the potential to trigger high antibody production in the host⁷. In addition, these nanoscale protein cages are non-pathogenic as they lack viral DNA and the ability to replicate making them a safer alternative in vaccine production as well as a promising platform for other nanomedical applications¹⁰. VLPs can be constructed rapidly and with relative ease using heterologous expression systems. Subsequently, VLPs can be modified using gene fusion techniques and chemical coupling protocols which makes them a versatile platform for both vaccine-based approaches as well as a cell-specific delivery platform¹¹.

Original success with VLP based technologies arose first with their use in vaccinology. In the 1980s, the discovery of the Hepatitis B Vaccine (HBV) surface antigen was the first successful VLP-based commercial vaccine⁶⁻⁸. The success of VLP-based vaccines persisted in the 2000s with the Human Papillomavirus (HPV) vaccines, Gardasil and Cervarix, which was created utilizing the HPV L1 capsid protein^{7,12}. Research in VLP-based vaccines continues to persist with current research evaluating their efficacy for preventing diseases such as Human Immunodeficiency Virus (HIV), Chikungunya, and influenza¹³⁻¹⁵. Success of VLP as a vaccine has lead to continued research into their efficacy as a cell-specific carrier of biologically active molecules.

VLPs are a promising platform for nanomedical applications due to their construction's adaptability and their compatibility with biological systems⁵. The ability for VLPs to be altered via genetic engineering and chemical modifications makes them an ideal candidate for cell

specific delivery of drugs and other molecules. The same principles governing the packaging of products naturally occurring in a viral capsid can be exploited to package other biologically active molecules including drugs or labeling molecules¹⁶. The highly repetitive surface geometry of VLPs also makes them ideal for the uniform addition of multiple surface motifs¹⁶. The chemical addition of glycopolymers and cell-penetrating peptides (CPPs) can be utilized to traffic modified VLPs to specific tissue types^{16,17}. VLP capabilities for internal drug loading as well as external cell targeting modifications, make these protein cages a potentially valuable tool in nanomedical applications including direct targeting of drugs to diseased tissue.

Nanomedicine

The majority of vaccines used currently rely on attenuated or inactivated forms of the virus which provoke an immune response in the patient, similar to that which would be provoked by the native virus¹⁸. Although these methods are highly affective, handling live viruses poses safety risks in their manufacturing and the potential for reversion into a live form introduces a additional potential risks in administration¹⁹. In efforts to increase the safety of vaccines, other methods including subunit based and DNA based vaccines were developed^{18,20}. These methods improved safety by eliminating the use of live viruses; however, these methods also posed several disadvantages including lack of immunogenicity, decreased efficacy, and potential safety concerns regarding foreign DNA²¹⁻²³.

The emergence of nanotechnology introduced a variety of nanocarrier platforms including liposomes, dendrimers, quantum dots (QDs) and VLPs subset of Virus Nanoparticles (VNPs)¹⁶. Applied potential uses for targeted nanocarrier platforms include a variety of medical applications as well as a potential tool for imaging²⁴. QDs, artificial semiconductor particles

ranging from 2-10nm, were originally thought to be a valuable imaging tool due to their persisting fluorescence, narrow emission spectrum, broad absorption spectra, and probe-like mechanism^{24,25}. However, compared to other methods they proved to be relatively cytotoxic²⁴. Similarly, Dendrimers, nanoscale artificial branching macromolecules capable of encapsulation, also exhibited *in vivo* toxicity^{24,26}. Liposomes are nanoscale phospholipid vesicles consisting of one or multiple concentric phospholipid bilayers which also have shown efficacy in drug trafficking *in vivo* but have failed to make the transition to clinical use²⁷. Major challenges to using liposomes as a drug trafficking strategy include rapid clearance by the Reticuloendothelial System (RES), opsinization, and Accelerated Blood Clearance (ABC) due to its synthetic properties^{24,27}.

VLPs, a subset of VNPs expressed in a heterologous system and lacking genomic material, are a potential solution for cell-specific trafficking of drugs and other molecules²⁴. VLPs emerged as a viable new vaccine technology due to their increased safety and immunogenicity¹⁸. Their success was first met in the 1980s with the origination of the first generation of the Hepatitis B vaccine (HBsAg)^{6,8,13}. The advance of VLPs as a new vaccine technology lead to more vaccines which more closely mimicked virion structure, including multiple vaccine for Human Papilloma Virus (HPV)¹³. Unlike previous models, the lack of viral DNA and inability to replicate renders them non-pathogenic and not at risk for reversion mutations¹⁸. This also eliminated the need for viral inactivation which is known to alter the presentation of important epitopes¹³. Continued research in VLPs as a potential vaccine technology has resulted in multiple successes in mammalian models including successful immunity for H7N9 and H5N1 influenza strains in mice and other viral diseases including hand, foot, and mouth disease (HFMD)²⁸⁻³¹. The success of VLPs *in vivo* and in clinical applications

has expanded research into discovery of their uses as a potential cell-specific nanocarrier platform.

VLPs are an ideal nanocarrier as compared to other competing systems due to their rapid construction, adaptability, and immunogenicity. VLPs can be easily produced in relatively large quantities due to their ability to self-assemble in vitro using bacterial and yeast cell hosts⁵. Additionally, they are highly adaptable and can be easily modified via genetic engineering and biochemical modifications³². These qualities make them ideal candidates for nanomedical applications as constructs can be rapidly tested and adapted as needed. In addition to their adaptability, VLPs are ideal due to their compatibility with biological systems. Naturally occurring properties of the viral capsid increase its immunogenicity as well as support its ability to enter cells^{9,12,33}. Their highly repetitive surface geometry mimics the structure of a native virus making them highly immunogenic¹³. VLPs have been shown to possess adjuvant properties which can initiate innate adaptive immune responses, including prolonged activation of the immune system through B cells^{5,10,13,34}. Their small size, 20-100nm, allows them to pass easily through the lymphatic system and the membranes of Antigen Presenting Cells (APCs)³⁴. VLPs also show a propensity for cell entrance similar to the natural functions of the virus⁹. Unmodified VLPs have been shown not to enter mammalian cells, while VLPs decorated with CPPs have been shown to enter cancerous cells³⁵. Biocompatibility of VLPs makes them an attractive potential solution for targeted drug delivery in many disease models including diseases which affect specific tissues such as cancers.

VLP HK97

This study utilizes Virus-Like Particle Honk Kong Isolate 97 (VLP HK97), a virus-like particle derived from a long-tailed bacteriophage and member of the *Siphoviridae* family which is known to infect *Escherichia coli*³⁶. The wild type capsid consists of 415 copies of the *gp5* coat protein which create its characteristic icosahedral structure. This particle is ideal for further experimentation due to its well characterized assembly and maturation, its highly stable structure, and its biocompatibility. This VLP can be synthesized in two variations. The first of which is made through heterologous expression of only the *gp5* coat protein which allows for the *in vitro* assembly of the HK97 pro-head structure which is approximately 60 nm in diameter³⁵. This form of the VLP is highly stable, however, a stronger capsid can be made through the heterologous expression of both the coat protein *gp5* and protease *gp4* *in vitro*. The protease allows for the formation of a highly stable catenane structure of cross-linked subunits which increases the strength of the protein cage^{17,37-40}. VLP HK97's well characterized development in addition to its highly repetitive surface geometry make it a good candidate for precise manipulation^{35,41-43}. Due to these characteristics, site specific genetic manipulations and chemical modifications can be carried out in a precise manner, including the external addition of CPPs and internal loading of drugs and other molecules.

VLP HK97s relative size, 30nm, also makes it an attractive platform. Compared to other site-specific technologies available, viral particles are relatively small, allowing for entrance into numerous cellular spaces. This increases the immunogenicity of these particles as they can actively drain into the lymph nodes and can accumulate in specific tissues^{6,8,44,45}. Relative to other VLPs of a similar size, VLP HK97 has a much larger internal space available for loading of drugs and other molecules. As compared to Cowpea chlorotic mottle virus (CCMV) and Red

clover necrotic mottle virus (*RCNMV*), two other VLPs currently under investigation, VLP HK97 has an internal capacity of $3.5 \times 10^7 \text{ \AA}^3$ ³⁵. This is approximately 9x larger than the internal capacity of CCMV and nearly 6.9x larger than RCNMV³⁵. Large amounts of internal space give VLP HK97 the potential to house high quantities of a given drug or molecule, allowing for less of the VLP itself to be administered.

Zebrafish: a complementary system for nanomedical applications of VLP HK97

The use of the zebrafish as a multifaceted vertebrate model organism was pioneered by geneticist George Streisinger in the 1960s⁴⁶. *Drosophila melanogaster* and *Caenorhabditis elegans* were the primary model organisms for genetics research at the time, however, a vertebrate organism was needed to move genetics research closer to the human model. In addition to being a useful model to genetics research, zebrafish lent themselves well to the field of developmental biology allowing for advances in nervous system development and patterning in the 1980s⁴⁶⁻⁴⁸.

Zebrafish lend themselves well to scientific experimentation due to their high fecundity and rapid development. At just 48 hours post fertilization (hpf) the segmentation period has been completed and development of the circulatory system and nervous system has already begun to occur⁴⁹. At 72hpf major organ systems of the body have been established and continue to mature⁴⁹. From five days post fertilization (dpf), major cartilaginous structures are established in the fish and can be visualized via staining^{49,50}. Their rapid and transparent development makes zebrafish highly efficient for laboratory testing.

In addition to its numerous advantages in the lab, its highly conserved genome has allowed zebrafish to serve as excellent vertebrate model for comparative research. With

approximately 70% of the zebrafish genome possessing a human ortholog, zebrafish serve as a useful platform for evaluating a variety of human diseases and disorders⁵¹. The zebrafish has also become a useful model for high-throughput testing for acute toxicity of a variety of molecules including surfactants, nanoparticles, and common teratogens^{50,52,53}. Meta-analyses of acute toxicity studies in zebrafish have also shown the results to be predictive of outcomes in mammalian models including common toxicity screens for rats and rabbits⁵⁴. The emerging body of work utilizing zebrafish as a high throughput platform for acute toxicity studies provides a platform for evaluation of novel drugs and foreign molecules, including VLPs. Because the synthesis of VLPs can be optimized to occur very quickly, capable of occurring in a matter of weeks, the zebrafish is ideal for equally rapid toxicity screens. The establishment of a baseline toxicity profile for unmodified VLP HK97 will allow for subsequent modifications of this particle, including the addition of CPPs, to also be assessed rapidly with a comparative baseline.

Ideal Disease Models for VLP HK97: Rhabdomyosarcoma

While many well characterized disease models in zebrafish could benefit from increased site selectivity of drugs, cancer treatments are an important area for research due to the widespread and aggressive side effects that are associated with these types of drug treatments. Depending on the type of cancer being treated, side effects can range from short term ailments such as nausea, vomiting, fatigue, and hair loss to long term or life threatening ailments including increased susceptibility to infection, memory loss and overall cognitive impairment, damage to the heart and nerves, and potential infertility^{2,55,56}. VLP based nanocarriers hope to alleviate these symptoms by trafficking the drug directly to the diseased tissue. This strategy aims to alleviate unwanted side effects in two ways: firstly, by avoiding entrance of the drug into

healthy cells and secondly, by decreasing the amount of drug that needs to be administered to the patient.

Rhabdomyosarcoma (RMS) is the most common soft tissue sarcoma in children and adolescents less than twenty years of age⁵⁷. Although the specific etiology of this cancer is unknown, it is thought to originate in striated muscle tissue and is found in two major subtypes, Embryonal Rhabdomyosarcoma (ERMS) and Alveolar Rhabdomyosarcoma (ARMS)⁵⁸. ERMS tumors generally develop in the head and neck or genital and urinary tracts. This subtype accounts for approximately 60% of all pediatric cancer diagnoses⁵⁹. Although prognosis for this cancer has improved, multiple factors contribute to treatment success rates including the primary tumor site, number of metastatic sites, and age of the patient⁵⁸.

A collection of RAS genes including H-RAS, K-RAS, and N-RAS are classified as proto-oncogenes with gain of function mutations observed in approximately 25% of all human cancers⁶⁰. These genes code for Ras proteins which govern cell proliferation, differentiation, and cell survival via the RAS/MAPK pathway⁶¹. Mutations in Ras genes can result in the over-proliferation of cells i.e. cancer⁶⁰. K-RAS is the most frequently mutated isoform accounting for 85% of RAS mutations and is typically mutated at codon 12^{60,62}. Moreover, activating mutations in Ras proteins including K-RAS mutations are associated with approximately 25% of ERMS patients⁵⁹. Commonly associated with ERMS and other sarcomas, inducing K-RAS activating mutations in zebrafish provide a working disease model for ERMS⁵⁹.

Characterized models of zebrafish embryonal rhabdomyosarcoma (zERMS) mimic human cancerous mutations and provide a relatively quick protocol for inducing tumorigenesis in the zebrafish model. Gene Set Enrichment Analysis and Microarray Analysis show high similarity to human ERMS with both morphological and clinical diagnostic similarities⁶³.

Tumorigenesis can be achieved with relative ease in zebrafish using a mosaic transgenic method with microinjection at the one-cell stage^{59,63}. Using this approach, tumor onset can be observed as soon as 10dpf, with an increase at 30dpf and 80dpf^{59,63}. Tumorigenesis occurs relatively quickly in the zebrafish as compared to conditional knock ins in murine models which can take as long as 300 days for tumor onset to occur depending on the system used⁶³. Zebrafish provide a highly functional and clinically similar model of ERMS which can be utilized to test potential targeted therapies like VLPs.

Currently, radiation and chemotherapy remain the first line of treatment along with localized surgical procedures⁶⁴. Systemic circulation of chemotherapeutics for treatment of this disease results in deleterious effects throughout the body in addition to their effects on cancerous cells. A Therapeutic Index (TI) is a metric which provides a comparison of the portion of therapeutic effect provided by a drug versus its toxic effects. Current TIs chemotherapeutics remain difficult to quantify due to the use of combination therapy for drugs and a lack of established concentration ranges^{65,66}. However, TI for current cancer treatments is estimated to be relatively low due to the vast side effects associated with cancer drugs. Application of VLPs in a cancer model could potentially increase the TI for commonly used chemotherapeutics for RMS due to cell-specific trafficking of the drug and increased immunogenicity provided by the VLP platform.

VLP Design Strategy

In order to utilize VLP HK97 as a potential delivery mechanism for a variety of disease models in zebrafish including zERMS, a baseline toxicity profile must be established to determine if components of the VLP may be cytotoxic. Initial toxicity experiments were

performed with unmodified VLP HK97. For localization experiments, Fluoroscien (FITC), a green fluorophore, was conjugated to the internal surface of the VLP for tracking via fluorescent microscopy. To test cell-specific targeting, a tripeptide motif Arg-Gly-Asp (RGD) was externally linked to VLP HK97.

The cell-specific trafficking strategy relies on the upregulation of RGD recognizing integrins on cancerous cells. Integrins are a family of cell-surface receptors which aid in cell interactions with the extracellular matrix. Bidirectional signaling pathways triggered by integrin binding serve a variety of functions including arrangement of the actin cytoskeleton and regulation of cell processes including differentiation, growth, and survival⁶⁷. Aberrations in integrin signaling observed in cancerous cells have been shown to promote cell survival and invasiveness as well as support the microenvironment which allows the tumor to grow and metastasize⁶⁸. Upregulation of integrin receptors has been shown to occur in many cancer types, making them an ideal site for cell-specific targeting⁶⁹. RGD specifically has been observed in binding eight distinct dimers of the integrin family, $\alpha v\beta 1$, $\alpha v\beta 3$, $\alpha v\beta 5$, $\alpha v\beta 6$, $\alpha v\beta 8$, $\alpha 5\beta 1$, $\alpha 8\beta 1$, and $\alpha IIb\beta 3$ ⁷⁰. This subgroup of receptors is influential in the functioning and metastases of cancerous tissue. Additionally, upregulation of several integrin subtypes has been observed in multiple cancer types including sarcomas^{71,72}.

Exploiting structural and physiological aberrations of cancerous tumors can also be used to increase the trafficking of a given chemotherapeutic to the desired target area. Vasculature characteristics unique to solid tumors include hypervascularization, increased permeability or blood vessels, and decreased lymphatic draining⁷³. The Enhanced Permeability and Retention (EPR) effect is a phenomenon observed in nanoscale molecules accumulating in cancerous tissue. This effect is believed to occur due to a variety of factors including the ability for these

particles to extravasate through the increased and leaky vessels in tumors and remain there due to decreased lymphatic drainage⁷⁴. However, it is necessary to mention that opinion in the field varies greatly on the true influence of the EPR effect in nanomedical applications in cancer. Cell-specific targeting of VLP HK97 to RMS tissue hopes to be accomplished via the RGD motif and exploitation of the EPR effect.

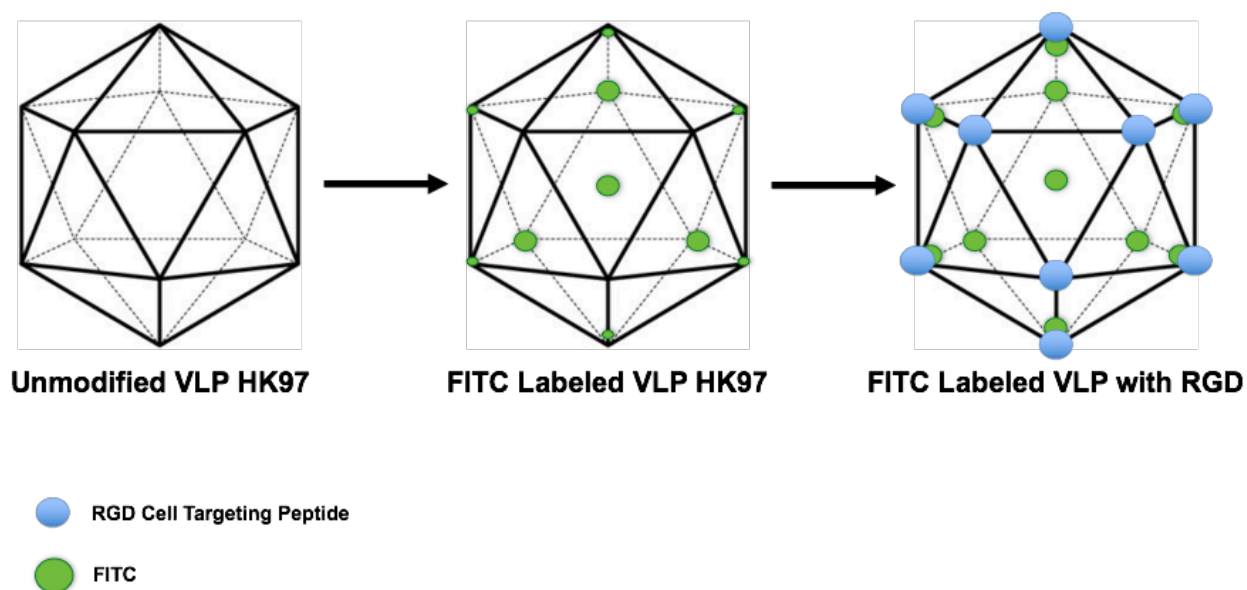


Figure 1. Design strategy for cell-specific targeting and localization of VLP HK97. Unmodified VLP HK97 (left) was internally loaded with FITC for localization via fluorescent microscopy (middle). Addition of the RGD motif (right) will drive the particle to cancerous tissue with upregulated integrin receptors

Chapter 2

Materials & Methods

Zebrafish Housing & Husbandry

Adult farm raised wild-type (WT) zebrafish were housed in a continuous flow circulating system (AHAB) and maintained on a 14-10 light/dark cycle at 28°C in reverse osmosis (RO) purified water (pH 7.4) salted with Instant Ocean Sea Salt to a salinity of 1.0 μ S⁷⁵. Fish are fed brine shrimp twice daily and kept in accordance with the University of Texas at Tyler IACUC protocol (IACUC Protocol #112).

For breeding, six zebrafish were placed in a breeding tank which allowed embryos to fall into a protected area for retrieval. All embryos used for experiments were kept in E3 medium and housed in a 28°C incubator⁷⁵.

Synthesis of VLP HK97

The synthesis of VLP HK97 and all modifications for these experiments were carried out by the Patterson Lab at the University of Texas at Tyler. HK97 VLPs were produced via heterologous expression in *E. coli* and subsequent purification via centrifugation and size exclusion chromatography (SEC) to isolate the desired product. Dynamic Light Scattering (DLS) was then used to confirm the identity of the desired product. Subsequent modifications include the internal loading of FITC. In addition, an RGD VLP HK97 was made by modification of the gene encoding GP5 with the RGD peptide sequence, which was subsequently labeled after purification for the studies in the same manner as WT VLP HK97.

Synthesis of *rag2:kRASG12D* & *rag2:DSRED*

Heterologous expression of *rag2:kRASG12D* and *rag2:DSRED* was carried out in *E.Coli*, provided by Dr. Eleanor Chen of the University of Washington. One colony of each bacterium was transplanted separately into 5ml of Luria Broth Media along with 10 μ l of Ampicillin. Cultures were incubated at 37°C for a maximum of 16 hours. Bacterial cells were harvested via tabletop centrifugation and plasmids were purified using the QIAGEN Plasmid DNA Purification Miniprep Kit. After purification, plasmids were linearized by restriction digest at the *XhoI* restriction site using the New England Biolabs Cutsmart protocol⁷⁶. Linearized DNA was then purified using the Monarch PCR & DNA Cleanup Kit. Isolation and linearization of the product was confirmed via Gel Electrophoresis. Concentration of each sample was determined via NanoDrop in ng/ μ l. Samples exceeding desired ranges for 260/280 and 260/230 ratios according to Thermo Scientific were excluded from use in experiments⁷⁷. Pure DNA was then diluted and used for injection in WT embryos. Original plasmids were obtained from the lab of Dr. Eleanor Chen.

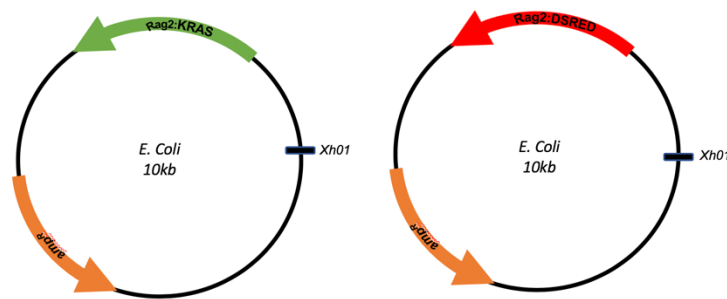


Figure 2. Plasmid maps depict the ampicillin resistant *E.coli* vector expressing either *rag2:KRAS12D* (left) or *rag2:DRED* (right) in addition to the *XhoI* restriction site.

Embryo Collection & Injection

Fertilized zebrafish embryos were collected within thirty minutes post fertilization initiated by the onset of a 14/10 light-dark cycle. For generation of tumors in WT zebrafish, increasing doses from 1.5 nl to 6.0 nl of ~80 ng/ μ l rag2:KRAS was injected into the single cell of the embryo using a microinjector and a PV830 Pneumatic PicoPump. Zebrafish were then incubated in E3 Medium and transferred to an AHAB system until mature⁷⁵.

Embryos for toxicity experiments were collected in the same manner and injected at the single cell stage into the yolk with VLP HK97 at increasing doses from 0 nl to 6.0 nl. A dosage curve was performed with pilot trials determining injection concentrations of 1.0 mg/ml, 0.75 mg/ml, 0.5 mg/ml, 0.25 mg/ml and 0.1 mg/ml VLP HK97. One-hour post injection, embryos were evaluated. Those not exhibiting cell division were removed, while other embryos were reserved and incubated at 28°C for further evaluation and experimentation⁷⁵.

Toxicity Profile

Viability Screening

The number of viable embryos were counted post injection at 0 dpf and again the following morning at 24 hpf. The mean viability for each trial dose was normalized to the viability of the controls for each biological replicate and then combined. Total mean viability was then determined for each dosage.

Morphological Toxicity

Multiple parameters of morphological toxicity were evaluated from 1 dpf to 5 dpf

according to standards established by previous acute toxicity assays and *Zebrafish: Methods for Assessing Drug Safety and Toxicity*⁵⁰. At 1 dpf through 5 dpf, all major structures including the head, eye, heart, tail, and yolk sac were examined for any major morphological aberrations. At 1 dpf, the morphological age of the larval fish was compared to its temporal age (24 hpf) to determine if any developmental delay was exhibited. At 3 dpf, presence or absence of melanocytes was recorded. At 4 dpf morphology of major structures previously mentioned was again monitored and recorded. At 5 dpf, larval zebrafish were fixed overnight in 4% paraformaldehyde on a benchtop rocking shaker. The following day, fish were stained in Alcian Blue following protocol retrieved from the Zebrafish Information Network (ZFIN)⁷⁸. Cartilaginous structures were then examined via bright field microscopy using a Zeiss Axioskop and imaged with a Sony digital camera.

Physiological Toxicity

At 3 dpf, the heartbeat of zebrafish was recorded for twenty seconds and extrapolated for a measurement in beats per minute (BPM). Measurements were normalized to the control for each biological replicate and then combined for each dosage.

Neural Toxicity

Central Nervous System functionality was examined via a “tap-elicited swim test” in which a small brush was used to graze the top of the head of each fish. A rapid aversion resulting in the fish swimming away from the stimulus was considered a “normal” response or non-toxic phenotype.

VLP HK97 Localization

Embryonic Localization

Zebrafish embryos were collected and injected into the yolk at single-cell stage with increasing doses of either 0.25 mg/ml VLP HK97:FITC or 0.25 mg/ml VLP HK97:FITC:RGD. Embryos were house in a 28°C incubator in E3 medium until 5hpf or the 50% epiboly stage. Embryos were mounted in 70% glycerol according to *The Zebrafish Book* protocol and analyzed using a Zeiss Light Scanning Microscope 5 Pascal⁷⁵. Entrance of the VLP from the yolk into the developing animal as well as uniformity of the distribution was monitored. Fluoresence was quantified using image J software⁷⁹.

Larval Localization

Larval zebrafish (2 dpf) were soaked in microcentrifuge tubes containing 3 nl of system water and 3 nl of either 0.25 mg/ml VLP HK97:FITC or 0.25 mg/ml VLP HK97:FITC:RGD. After two hours of soaking, larval zebrafish were removed from the microcentrifuge tubes and imaged via fluorescent microscopy using a Zeiss LSM 5 Pascal microscope.

Adult Localization

Adult zebrafish were soaked overnight in a 1:50 ml dilution of ~2.0 mg/ml VLP HK97:FITC in system water. The following morning zebrafish were euthanized in cold water according to (IACUC Protocol #112). Zebrafish were then set in a 7% agarose block and nine transverse cuts were made from the anterior to posterior axis of the fish (Figure 3). Dorsal and ventral regions of individual sections were

then imaged using a Zeiss LSM 5 Pascal confocal microscope. Fluorescence of these images were analyzed and quantified using Image J software⁷⁹.

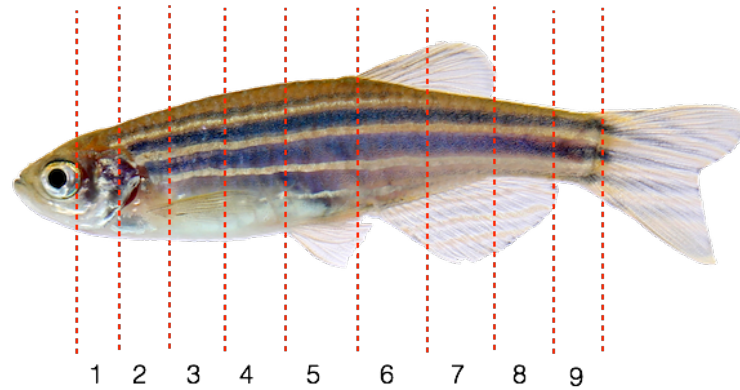


Figure 3. Sectioning schema for adult zebrafish treated with VLP HK97.

Data Analysis

Data and images were analyzed using the following software programs: Microsoft Excel for Mac Version 16.20, GNU Image Manipulation Platform (GIMP), and Graph Pad Prism for Windows⁸⁰⁻⁸².

Chapter 3

Results

Toxicity Profile

Farm-raised WT zebrafish embryos were collected and injected into the yolk with varying concentrations of VLP HK97 at the one cell stage. Embryos were kept in E3 medium in a 28°C incubator and observed daily until 5 hpf. Viability, morphology, as well as physiological and behavioral parameters were measured and recorded daily to establish baseline toxicity for unmodified VLP HK97.

Viability Screening

Embryonic Viability at 24 Hours Post Injection of Unmodified VLP HK97

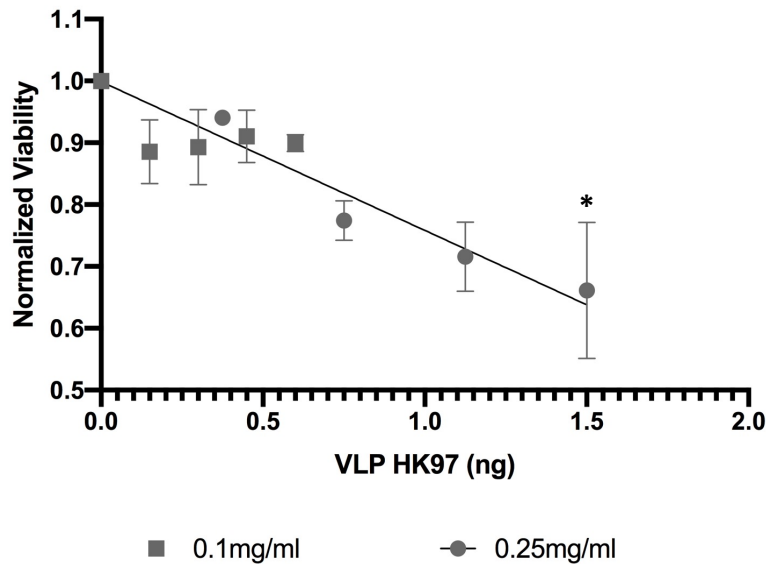


Figure 4. Viability of embryos at 1 dpf following injection of unmodified VLP HK97 at 0.1 mg/ml and 0.25 mg/ml. 0.25 mg/ml: $F(4,17) = 4.510$, $P=0.0290$ * = 0.0404. 0.1 mg/ml: $F(4,10) = 2.518$, $P=0.1077$

At an injection concentration of 0.25 mg/ml VLP HK97, an inversely proportional relationship between injection volume and viability is observed. Four biological replicates were recorded with approximately 30 embryos per group per injection dose. Biological replicates were normalized to their respective controls and then grouped for analysis. At this concentration, a linear relationship was observed and an LD50 of 2.08ng was extrapolated from a linear regression. An adjusted dose of 0.1 mg/ml was also tested. Three biological replicates were observed with approximately 50 embryos per injection dose. Biological replicates were normalized to their respective controls and then grouped for analysis. An average viability of 89% across at 1dpf was observed across all injected embryos. With a minimum of 88% and a maximum of 91% viability observed.

Embryonic Viability at 24 Hours Post Injection of VLP-FITC-RGD

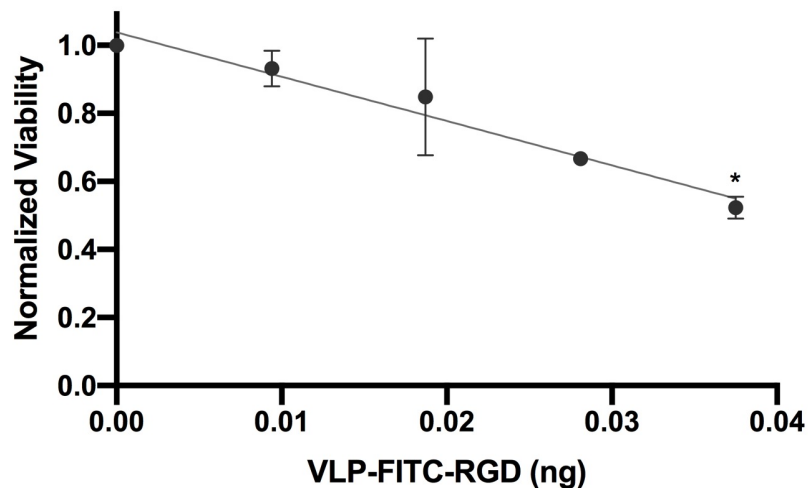


Figure 5. Viability measures after the addition of the RGD cell targeting peptide decreases the amount of VLP that can be injected before reaching the LD50 of 0.0413ng. $F(4,5)=10.46$ $P=0.0120$ $*=0.0130$

Single celled embryos injected with increasing doses of VLP HK97:RGD:FITC. A linear regression allows for the extrapolation of an LD50 of 0.0413ng.

Morphological Toxicity

Developmental Delay at 24hpf of Zebrafish Injected with Unmodified VLP HK97

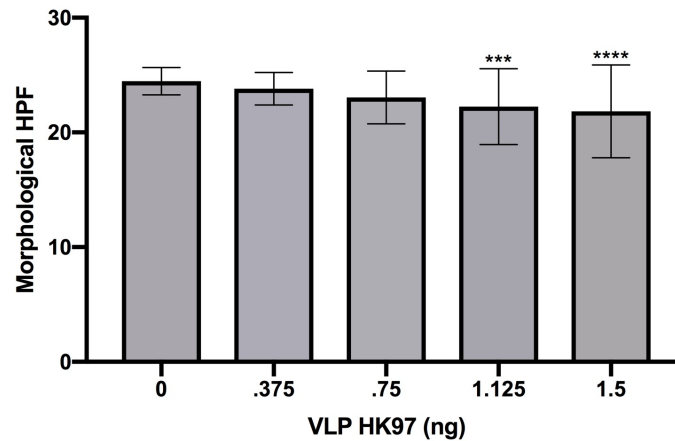


Figure 6. Developmental delay measured by assessing morphological age is not observed in larval zebrafish injected with increasing doses of 0.25mg/ml unmodified VLP HK97 at the one cell stage. 0.25mg/ml: $F(4,208) = 8.244$, $P < 0.0001$ *** = .0005 **** = <.0001

Larval zebrafish were observed at 24 hpf. Their temporal age was compared to their morphological age using the developmental clock provided by *The Zebrafish Book* as a metric⁷⁵. Discrepancies in morphological age from temporal age indicate developmental delay. 10 embryos were examined for each dose and three biological replicates were examined. Each biological replicate was normalized to their respective control and combined for analysis. At an injection concentration of 0.25 mg/ml VLP HK97, a significant decrease in morphological age was observed in treated fish beginning at a dose of 1.125 ng VLP HK97 ($P < 0.0001$). At the adjusted concentration of 0.1 mg/ml VLP HK97 all fish were recorded as having a morphological age of 24 hpf indicating no developmental delay.

Tail Deformities in Zebrafish Injected with Unmodified VLP HK97

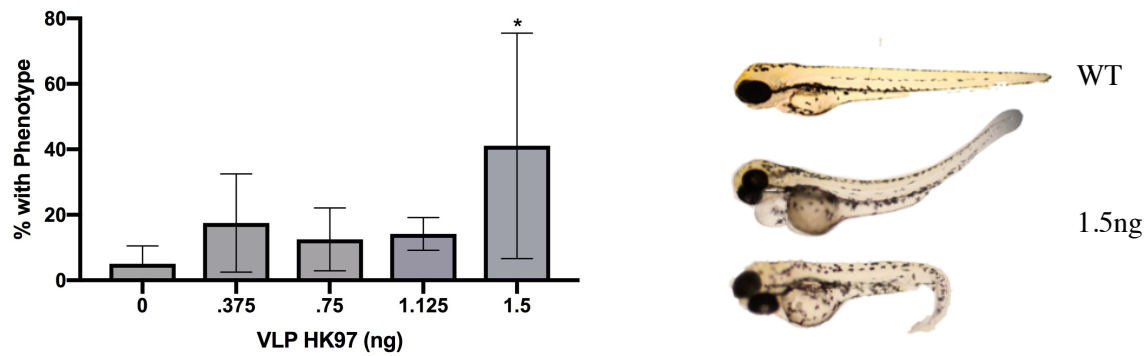


Figure 7. Tail deformities are observed at the highest injection dose (1.5ng) at 1dpf after injection of increasing doses of 0.25mg/ml unmodified VLP HK97, $F(4,17)=2.892$, $P=0.0539$ * = 0.0285 (left) . No toxic phenotypes are observed at all other injection doses(left). Two fish exhibiting tail deformities after injection with 1.5ng VLP HK97 as compared to WT controls (right).

At 1dpf, ten larval zebrafish were randomly selected from each injection volume and subsequently dechorionated. Three biological replicates were observed and normalized to their respective controls before being combined for data analysis. Larval fish were examined for morphological aberrations including tail deformities. At an injection concentration of 0.25 mg/ml VLP HK97, a significant increase in tail deformities was only observed at the highest injection volume, 6.0nl (1.5ng VLP HK97) ($P=0.0285$). Uniformity in tail aberrations was not observed. Both forward and backward bends were observed. At the adjusted dose of 0.1 mg/ml VLP HK97, no tail deformities were observed across trials.

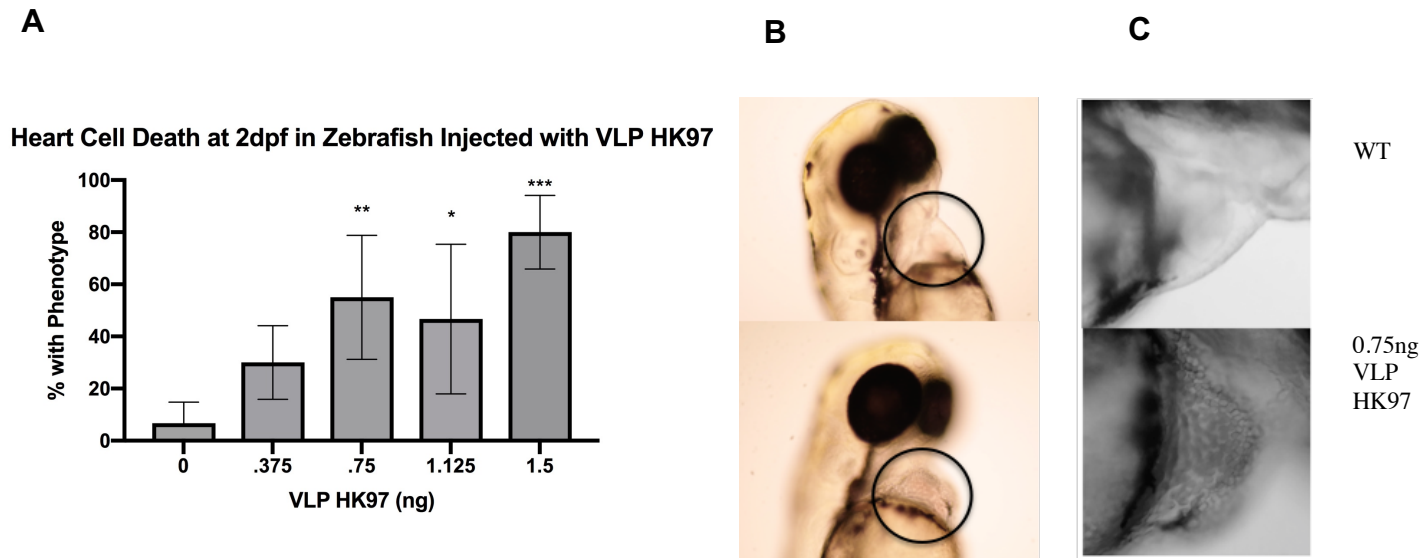


Figure 8. Pericardial cell death is observed at high injection observed at 2dpf after injection of 0.25mg/ml unmodified VLP HK97 at the one cell stage, 0.25mg/ml: $F(4,17)=9.044$ $P=0.004$ $*=0.0261$ $**=0.0046$ $***=0.003$ (A). Bright field images of the heart and pericardial region of WT and treated fish. Magnification of the heart and pericardial region (C).

At 2 dpf, ten larval zebrafish from each injection dose were randomly selected, dechorionated, and observed for various morphological aberrations. At an injection concentration of 0.25 mg/ml unmodified VLP HK97, a significant increase in clouding in the pericardial region, assumed to be cell death, was observed in treated fish beginning at an injection volume of 3.0 nl (0.75 ng VLP HK97) and continuing to the highest injection volume, 6.0 nl (1.5 ng VLP HK97) ($P=0.004$). The circled region indicates the heart and pericardial region of the larval zebrafish (B) in addition to a magnified view of this same region (C). At the adjusted dose of 0.1 mg/ml, no significant increase in pericardial cell death was observed across doses, $F(4,10)=0.6250$ $P=0.6554$.

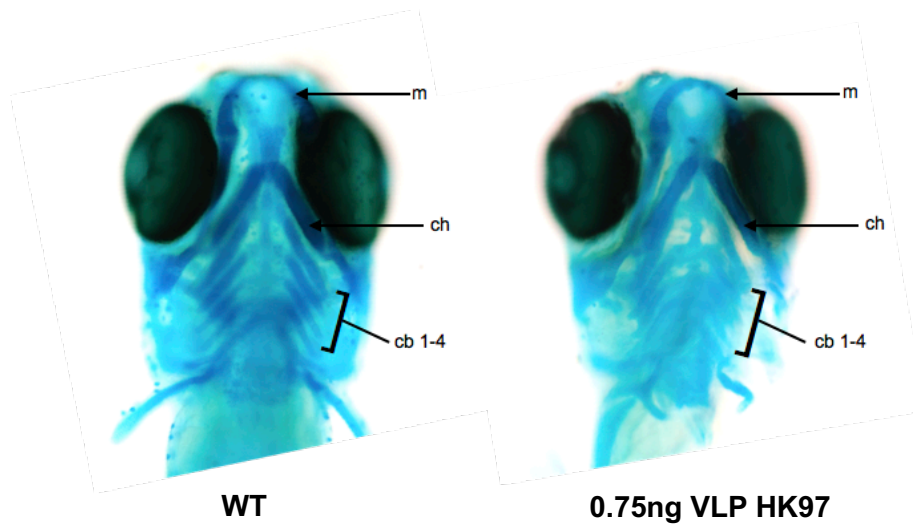


Figure 9. Alcian blue stain reveals no deformities of major cartilaginous structures in zebrafish at 5dpf after injection of unmodified VLP HK97 at the one-cell stage shows no toxic phenotype in treated fish. Meckel's structures (m), Ceratohyal (Ch), and Ceratobranchial (Cb) structures are noted.

At 5 dpf, ten zebrafish from each injection dose were randomly selected, euthanized and fixed in 4% paraformaldehyde solution overnight and subsequently stained in Alcian Blue for observation of cartilage in the larval zebrafish. Zebrafish were then observed using bright field microscopy for any differences in cartilage development across trials. Major structures shown here include Meckel's second arch structures (m), Ceratohyal (Ch), and Ceratobranchial (Cb) structures. Qualitative analysis indicates no differences in cartilaginous structures of developing zebrafish between treated fish and uninjected controls (n= 50).

Physiological Toxicity

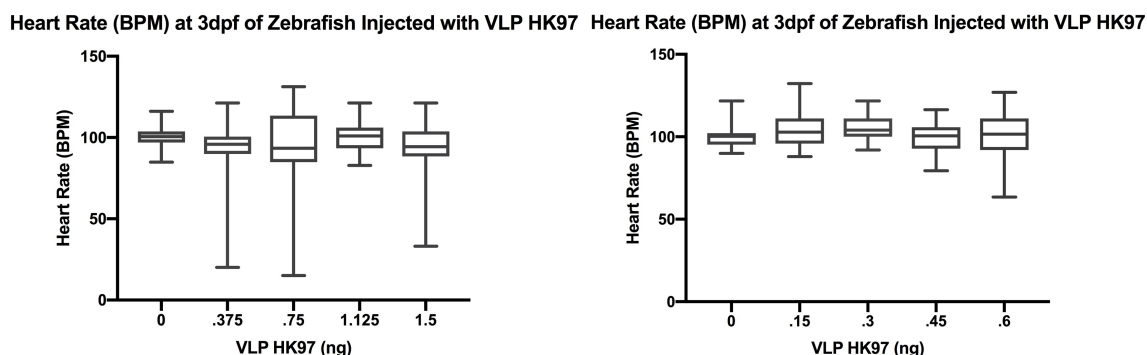


Figure 10. Injection of unmodified VLP HK97 at increasing dosages shows no toxic effects on heart rate in *Danio rerio*. 0.25 mg/ml $F(4,207)=2.602$ $P=0.0371$ (left). 0.1 mg/ml $F(4,143)=1.701$ $P=0.1530$ (right).

At 3 dpf, ten zebrafish from each injection volume were randomly selected, dechorionated, and heart rate (HR) in beats per minute (BPM) was recorded. Three biological replicates were observed and data was normalized to their respective controls and subsequently combined for analysis. At an injection concentration of 0.25mg/ml unmodified VLP HK97, no significant difference in HR was observed between uninjected controls and treated fish. Similarly, at the adjusted concentration of 0.1mg/ml unmodified VLP HK97, no significant difference in HR was observed between treated fish and uninjected controls.

Neural Toxicity

All zebrafish injected with increasing doses (0nl -6.0nl) of 0.25mg/ml unmodified VLP HK97 passed the tap-elicited swim test resulting in a positive response (n=30). All zebrafish injected with increasing doses of 0.1mg/ml VLP HK97 also passed the tap-elicited swim test resulting in a positive response (n=30).

Summary of Toxicity Profile of Unmodified VLP HK97

	Developmental Delay	Tail Deformity	Eye Deformity	Pericardial Cell Death	Heart Rate Aberrations	Tap-elicited Swim Test	Craniofacial Malformations
0.1 mg/ml	not observed	not observed	not observed	not observed	not observed	not observed	not observed
0.25 mg/ml	observed \geq 1.125 ng	observed \geq 1.5 ng	not observed	observed \geq 0.75 ng	not observed	not observed	not observed

Table 1. Summary of the toxicity profile indicates no toxic phenotypes are observed at biologically relevant doses of unmodified VLP HK97. Two concentrations in the dosage curve are highlighted, 0.25mg/ml and 0.1mg/ml.

VLP HK97 Localization

Embryonic Localization

Localization of VLP HK97:FITC in 5 dpf Zebrafish Embryos

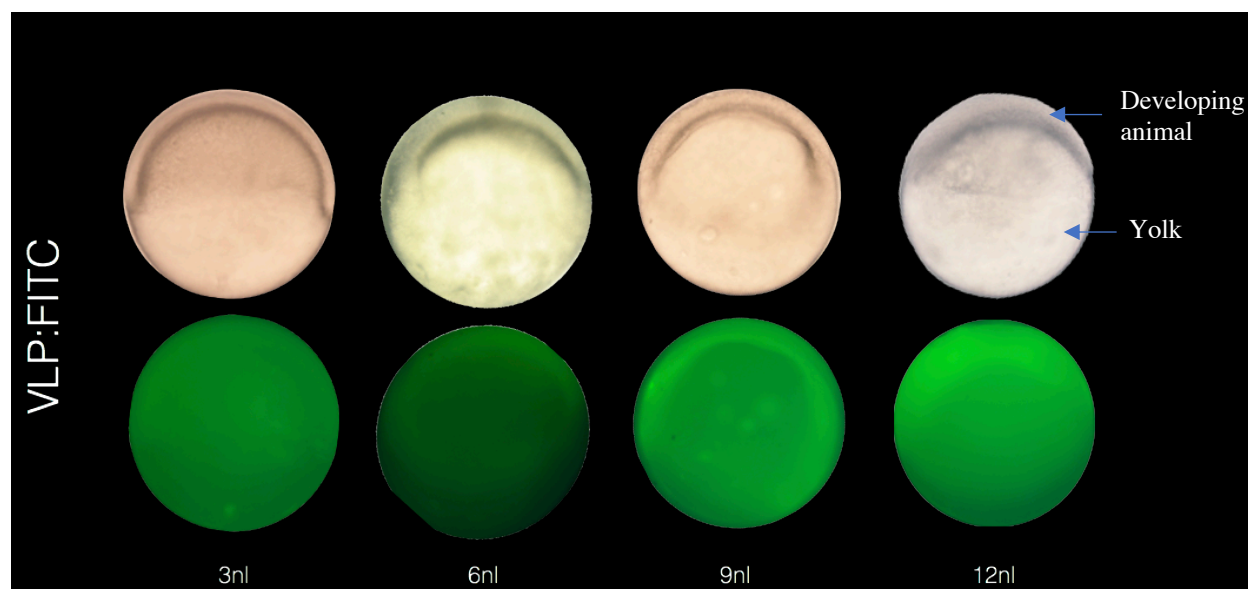


Figure 11. Injection of single cell embryos with FITC labeled VLP HK97 shows uniform entrance of the particle into the developing tissue of the animal (bottom). Bright field images of each embryo are also provided (top).

Zebrafish embryos were injected into the yolk with varying doses of 0.25 mg/ml VLP HK97:FITC at the one cell stage. Embryos were stored in a 28°C incubator until 5 hpf or 50% epiboly was reached. At 5 hpf, embryos were analyzed using bright field and fluorescent microscopy. Bright field images (Figure 11, top) of the 5 hpf embryos are shown along with the fluorescent image of the same embryo (Figure 11, bottom). Images indicate entrance of the nanoparticle into the tissue of the developing embryo from the yolk.

Localization of VLP HK97:FITC:RGD in 5 dpf Zebrafish Embryos

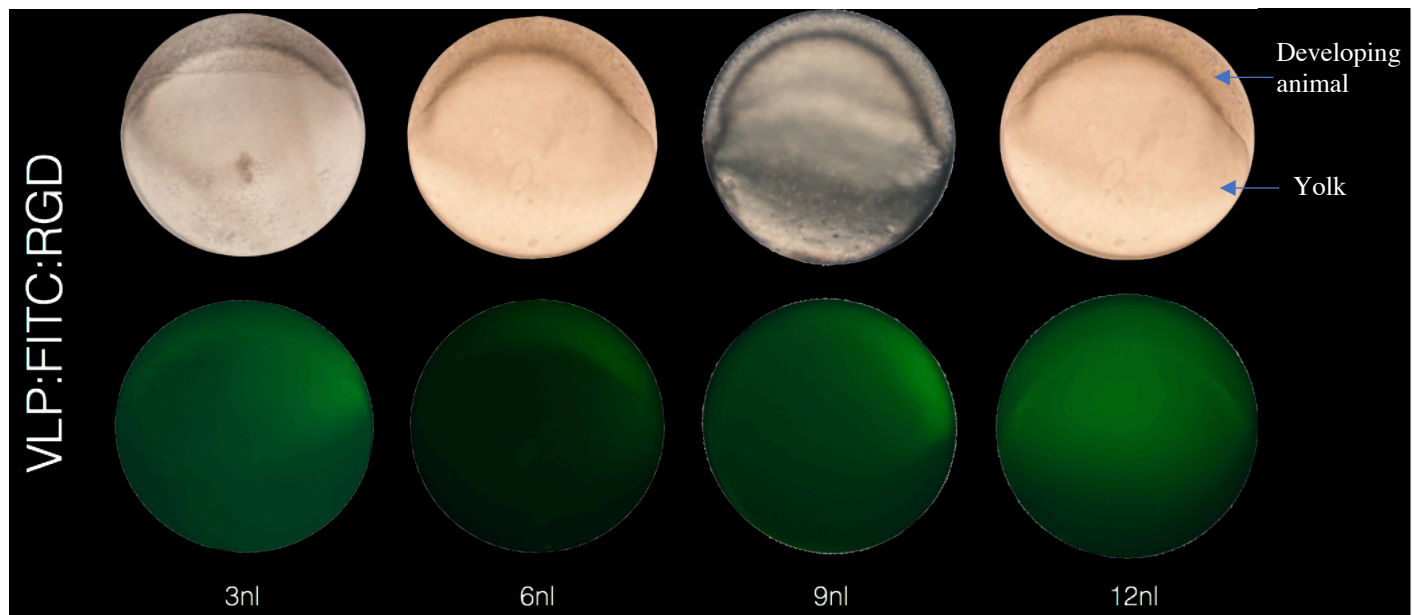


Figure 12. The addition of the RGD cell targeting peptide results in non-uniform entrance of the particle into developing tissue of the animal (bottom). Corresponding bright field images of the 5hpf embryos (top).

Non-uniform Distribution of VLP:FITC:RGD in Developing Zebrafish Embryos

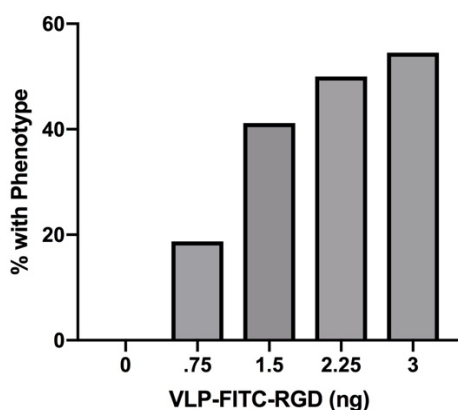


Figure 13. Percentage of embryos which exhibit non-uniform distribution of VLP HK97:FITC:RGD in the developing animal.

Zebrafish embryos were injected into the yolk with varying doses of 0.25 mg/ml VLP HK97:RGD:GFP at the one cell stage. Embryos were stored in a 28°C incubator until 5 hpf or 50% epiboly was reached. At 5 hpf, embryos were analyzed using bright field and fluorescent microscopy. Bright field images (Figure 12, top) of the 5 hpf embryos are shown along with the fluorescent image of the same embryo (Figure 12, bottom). Images indicate entrance of the nanoparticle into the developing tissue from the yolk. Non-uniform grouping of the nanoparticle is also observed in the lateral portions of the developing tissue.

Larval Localization

Larval zebrafish (2 dpf) were soaked for two hours in 0.25 mg/ml VLP HK97:FITC:RGD and subsequently imaged via fluorescent microscopy. Results indicate localization of the particle to known areas of integrin expression in larval zebrafish.

Localization of VLP HK97:FITC in 2 dpf Larval Zebrafish

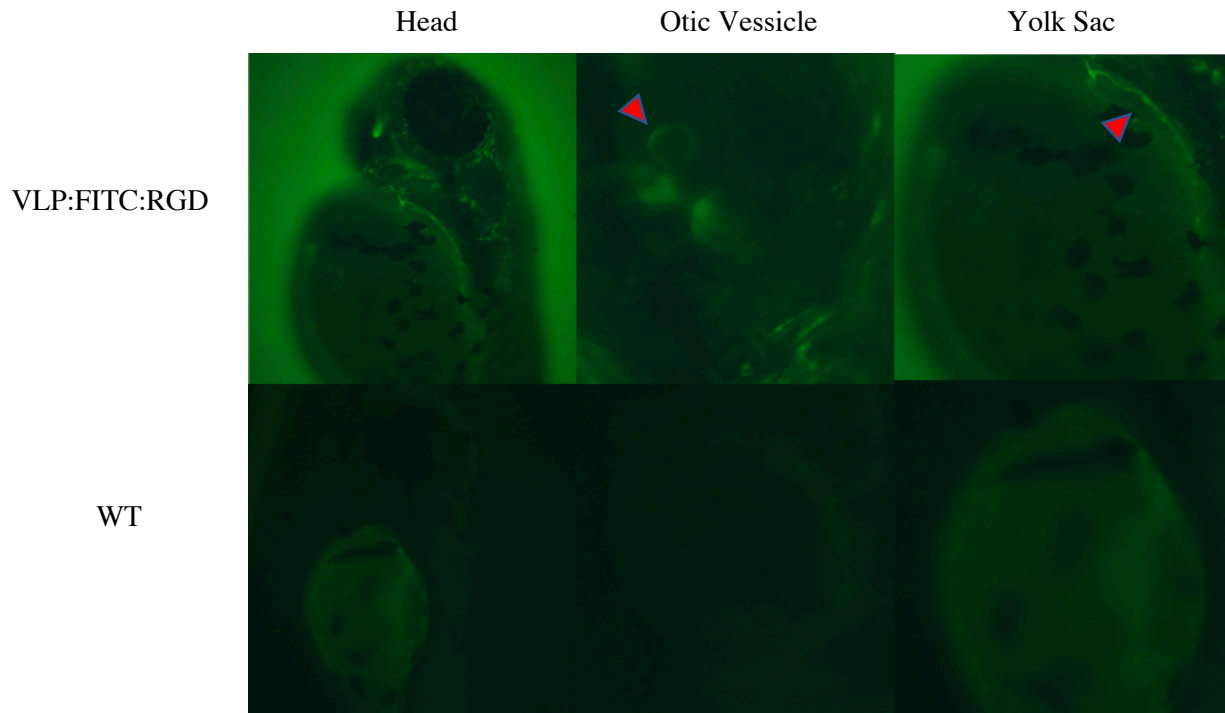


Figure 14. VLP HK97:FITC:RGD localizes to known regions of integrin expression in larval zebrafish including the otic vesicle and junction between the yolk sac and developing animal.

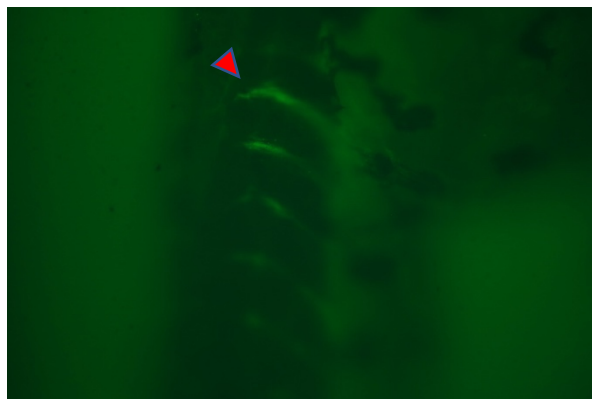


Figure 15. VLP HK97:FITC:RGD localizes to known regions of integrin expression in larval zebrafish including the somites.

Adult Localization

Mean Pixel Intensity of Transected Adult Zebrafish Treated with VLP HK97:FITC

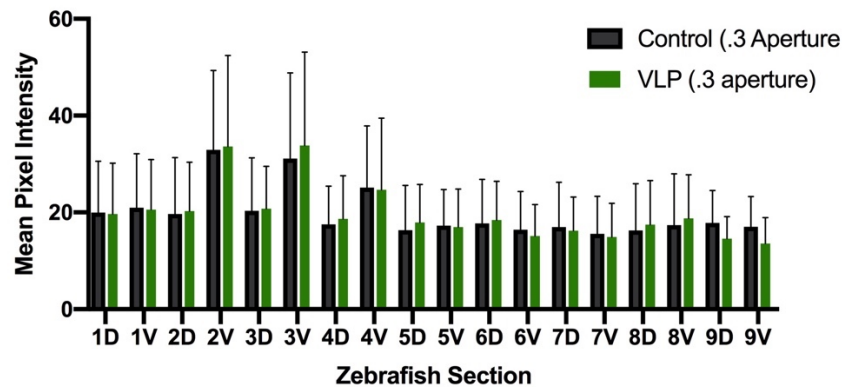


Figure 16. VLP HK97 does not localize to specific body regions after overnight treatment in adult zebrafish

No significant difference is observed across sections, dorsal (D) and ventral (V), between treated fish and untreated controls.

zRMS Tumorigenesis



Figure 17. Successful induction of tumorigenesis (circled) in zebrafish using linearized KRAS vectors.

Farm-raised WT zebrafish embryos were injected with linearized rag2:KRAS DNA to drive the formation of RMS tumors in the tail region of the zebrafish. Through this method tumorigenesis was observed indicated by the circled regions.

Chapter 4

Discussion

VLPs provide a promising new platform for cell-specific targeting of drugs and other molecules due to their ease and safety in preparation, natural immunogenic properties, and inherent biocompatibility. Establishing a basis for testing VLPs and their various modifications in zebrafish will provide a complementary platform for VLPs to be modified and tested rapidly in the wide variety of disease models characterized in *Danio rerio*.

Toxicity Profile

Unmodified VLP HK97

A comprehensive baseline toxicity profile of VLP HK97 in *Danio rerio* reveals that unmodified VLP HK97 is non-toxic at below the dose of 0.75ng (Table 1). *In vitro* studies evaluating entrance of unmodified VLP HK97 in Hela cell and mouse fibroblast lines also did not report cytotoxicity of the particle³⁵. Viability assays reveal an LD50 of 2.08ng VLP HK97 with toxic effects only being observed at high doses of 0.25 mg/ml VLP HK97 (Figure 4). An adjusted concentration of 0.1 mg/ml VLP HK97 shows no significant difference in viability between treated fish and uninjected controls (Figure 4). Examination of morphological characteristics of major structures in larval zebrafish up to 5 dpf indicate that unmodified VLP HK97 induces little to no toxic effects in the zebrafish at biologically relevant doses (Figure 6-10). Toxic phenotypes including tail deformities and pericardial cell death were observed, however only at high doses of 0.25 mg/ml VLP HK97 (Figure 7-8). Physiological and neural toxicity parameters indicate no significant differences between treated fish and uninjected controls (Figure 10). Other *in vivo* toxicity studies using other non-mammalian derived VLPs

like *cowpea mosaic virus* (CPMV) have shown doses up to 100mg/kg of body weight to be non-toxic in mouse models⁸³. On average, a dry larval zebrafish has been recorded to weigh between 58 and 79 μg when measured across multiple time points from 0 hpf to 96 hpf⁸⁴. These time points used for weight measurements mimic the time frame used for toxicity assays in this study. From these biometrics, it is inferred that a range of 1.29 ng/ μg to 0.95 ng/ μg is not toxic in zebrafish across the time points examine (0 hpf – 96 hpf). This baseline toxicity profile establishes VLP HK97 as a promising candidate for cell specific delivery as it is non-toxic at biologically relevant doses in *Danio rerio*.

VLP HK97:FITC:RGD

VLP HK97:FITC:RGD is toxic to larval zebrafish beginning at much lower doses than the unmodified particle (Figure 5). In conjunction with localization experiments, it can be inferred that a nonuniform dispersal of the particle may be causing this result. Trafficking of the particle to cells expressing integrin receptors in the early stage embryo may be causing the collection of VLP HK97 in specific cell types rather than diffusing throughout the embryo. This agrees with the hypothesis that increased localization will decrease the amount of drug needed to be administered to a patient. Co-localization assays should be performed to confirm the modified VLP in localizing to known integrin subtypes in the embryonic zebrafish.

In zebrafish models with diseased tissue, RMS for example, it is hypothesized that VLP HK97:FITC:RGD will be driven towards the cancerous tissue with upregulated integrin receptors⁸⁵. Upregulation of the integrin receptors will create a preference for the modified VLP to enter the cancerous cells, increasing the site selectivity of the encapsulated chemotherapeutic

agent. This will result in an increase in the amount of target tissue reached and drug released thus decreasing the amount of VLP that needs to be administered initially.

Cytotoxicity of the modified particle may be another potential explanation for the decreased LD50 of VLP-RGD. A previous *in vitro* study concluded that unmodified VLP HK97 did not interact with Hela Cells or mouse fibroblast cells³⁵. Upon the addition of the cell-targeting peptide, transferrin (tf), the VLP was uptaken into both cell lines with a preference for the Hela cells³⁵. Further assays must be performed to determine if the RGD peptide is directly responsible for cytotoxicity in the zebrafish embryos.

VLP HK97 Localization

Embryonic Localization

Embryonic injection of VLP HK97:FITC and analysis at 5 hpf indicate entrance of the nanoparticle into the developing tissue from the initial injection site in the yolk of the embryo. Uniform entrance of VLP HK97:FITC into the developing tissue of the embryo is also observed (Figure 11). This indicates that unmodified VLP HK97 can be injected into the yolk at the one cell stage and easily pass into the developing tissue. This is beneficial for both research and clinical applications. In the research setting, yolk injections are often easier and quicker to achieve than direct cell injections. Injection of future VLPs and their modifications can be tested more efficiently and accurately via simple yolk injections. These findings are also clinically relevant because they indicate no preference for unmodified VLP HK97 into specific tissues. This provides an unbiased platform which can then be driven to specific cell types by utilizing cell targeting peptides affixed to the external surface of the VLP.

Repetition of this assay utilizing VLP HK97:FITC:RGD indicates non-uniform entrance of the particle from the yolk into the developing tissue (Figure 12). We hypothesize the addition of the cell targeting peptide is driving the particle to accumulate in specific subsets of cells beginning in the early embryo. Most notably, at a 12 nl injection volume a collection of the particle is observed at the junction between the yolk and the developing animal which is a known site of integrin expression in embryonic zebrafish⁸⁶.

Larval Localization

Soaking larval zebrafish in VLP HK97:FITC:RGD helped to confirm localization results found in embryonic zebrafish. Distinct regions of localization of the particle are observed in the head region of the fish which was not observed in WT zebrafish (Figure 14). The RGD motif affixed to the external surface of the VLP is known to bind over twenty integrin subtypes including $\alpha v\beta 3$, $\alpha v\beta 5$ and $\alpha 5\beta 1$ ^{70,85,87,88}. The vast binding capability of RGD to multiple integrin subtypes makes it a promising candidate for targeting cancerous cells and multiple integrin subtypes have been shown to be upregulated in a variety of different cancer types⁶⁹. Individual cancer cell types can also express integrin subtypes differentially⁶⁸. This has been shown to be true of sarcomas specifically with beta subtypes⁷². Characterizing the zRMS tumors and determining which integrin receptors are dysregulated is a key step to moving forward with using RGD as a CPP in this model.

Most notably in these experiments, increased localization is seen in known areas of integrin expression in larval zebrafish including the otic vesicles, somite borders, and the junction between the yolk and developing animal which was mimicking in embryonic assays (Figure 14-15)⁸⁶. Localization seen in this study mimics *in situ* studies identifying areas of

integrin expression in larval zebrafish^{78,86}. These findings indicate that the RGD motif may be a promising candidate for directing the particle to cancerous cells with upregulated integrin receptors. Colocalization assays should be done to ensure that areas of particle localization overlap areas of integrin expression at different time points in the zebrafish life cycle.

Adult Localization

Unmodified VLP HK97:FITC was administered adult zebrafish via soaking overnight. Treated zebrafish were subsequently euthanized and sectioned and analyzed using fluorescent microscopy (Figure 3). Analysis of the fluorescence intensity reveals no significant difference between WT controls and treated fish (Figure 16). Initial examination indicates that accumulation of the unmodified particle is not occurring in any specific tissue or transection. However, variation in data points among controls indicates this method may not be effective for assessing fluorescence comparatively. Issues with autofluorescence due to tissue shearing may be causing these results. Other sectioning methods that prevent tissue shearing could be potential solutions to this problem. Further analysis including additional time points is needed to determine if the particle could potentially accumulate if left for a longer period of time in the adult zebrafish.

Rhabdomyosarcoma Model in Zebrafish

Tumors were successfully generated through direct cell injections of rag2:KRAS DNA (Figure 17). This method will provide a model to assess the efficacy of RGD as a candidate for trafficking VLPs to cancerous tissue.

Currently, expression of various integrin subtypes has begun to be characterized in zebrafish however full profiles of integrin expression in early stage embryos have not been completed⁷⁵. Further exploration of integrin expression in early stages is needed to assess targeting of VLP HK97:FITC:RGD. Further characterization of the zebrafish RMS model is also needed to increase the efficacy of VLP targeting as well as the accuracy of these assessments. Identifying key integrin subtypes upregulated in this particular model will provide insight into the site selectivity that could be achieved via RGD in this model. If upregulation of specific integrin subtypes are identified in this specific cancer model, the potential for a more finely tuned VLP may arise through targeting of specific integrin subtypes.

Application of the targeted VLP HK97:RGD in the zRMS model is also necessary to assess the efficacy of the nanoparticle as a potential drug delivery system. These experiments have shown this VLP's propensity for cell entrance and the potential for RGD as an efficacious cell-targeting peptide. Accumulation of this particle in cancerous tissue in the zRMS model would indicate integrin receptors are a feasible target for trafficking these particles to disease tissue and avoiding death of healthy cells.

References

- 1 Huggins, D. J., Sherman, W. & Tidor, B. Rational approaches to improving selectivity in drug design. *J Med Chem* **55**, 1424-1444, doi:10.1021/jm2010332 (2012).
- 2 (ed Patient Education Brochures Harvard Health Publications) (Harvard Health Publications, Boston, MA, 2016).
- 3 Society, A. C. *How Chemotherapy Drugs Work*, (2016).
- 4 Society, A. C. *Chemotherapy Side Effects*, (2016).
- 5 Chroboczek, J., Szurgot, I. & Szolajska, E. Virus-like particles as vaccine. *Acta Biochim Pol* **61**, 531-539 (2014).
- 7 Zeltins, A. Construction and characterization of virus-like particles: a review. *Mol Biotechnol* **53**, 92-107, doi:10.1007/s12033-012-9598-4 (2013).
- 8 Mona O. Moshen, L. Z., Gustavo Cabral-Miranda, Martin F. Bachmann. Major findings and recent advances in virus-like particle (VLP)-based vaccines. *Seminars in Immunology* **34**, 123-132, (2017).
- 9 Zdanowicz, M. & Chroboczek, J. Virus-like particles as drug delivery vectors. *Acta Biochim Pol* **63**, 469-473, doi:10.18388/abp.2016_1275 (2016).
- 10 Mohsen, M. O., Gomes, A. C., Vogel, M. & Bachmann, M. F. Interaction of Viral Capsid-Derived Virus-Like Particles (VLPs) with the Innate Immune System. *Vaccines (Basel)* **6**, doi:10.3390/vaccines6030037 (2018).
- 11 Pumpens, P., Ulrich, R., Sasnauskas, K., Kazaks, A., Ose, V., & Grens, E. Construction of novel vaccines on the basis of the virus-like particles: Hepatitis B virus proteins as vaccine carriers. *Medicinal protein engineering*, 205-248 (2009).
- 12 Wang, J. W. & Roden, R. B. Virus-like particles for the prevention of human papillomavirus-associated malignancies. *Expert Rev Vaccines* **12**, 129-141, doi:10.1586/erv.12.151 (2013).
- 13 Roldao, A., Mellado, M. C., Castilho, L. R., Carrondo, M. J. & Alves, P. M. Virus-like particles in vaccine development. *Expert Rev Vaccines* **9**, 1149-1176, doi:10.1586/erv.10.115 (2010).
- 14 Saraswat, S. *et al.* Expression and Characterization of Yeast Derived Chikungunya Virus Like Particles (CHIK-VLPs) and Its Evaluation as a Potential Vaccine Candidate. *PLoS Negl Trop Dis* **10**, e0004782, doi:10.1371/journal.pntd.0004782 (2016).
- 15 Wu, P. *et al.* Single Dose of Consensus Hemagglutinin-Based Virus-Like Particles Vaccine Protects Chickens against Divergent H5 Subtype Influenza Viruses. *Front Immunol* **8**, 1649, doi:10.3389/fimmu.2017.01649 (2017).
- 16 Ma, Y., Nolte, R. J. & Cornelissen, J. J. Virus-based nanocarriers for drug delivery. *Adv Drug Deliv Rev* **64**, 811-825, doi:10.1016/j.addr.2012.01.005 (2012).
- 17 van Kan-Davelaar, H. E., van Hest, J. C., Cornelissen, J. J. & Koay, M. S. Using viruses as nanomedicines. *Br J Pharmacol* **171**, 4001-4009, doi:10.1111/bph.12662 (2014).
- 18 Fuenmayor, J., Godia, F. & Cervera, L. Production of virus-like particles for vaccines. *N Biotechnol* **39**, 174-180, doi:10.1016/j.nbt.2017.07.010 (2017).
- 19 Ulmer, J. B., Valley, U. & Rappuoli, R. Vaccine manufacturing: challenges and solutions. *Nat Biotechnol* **24**, 1377-1383, doi:10.1038/nbt1261 (2006).

- 20 Schiller, J. T. & Lowy, D. R. Raising expectations for subunit vaccine. *J Infect Dis* **211**, 1373-1375, doi:10.1093/infdis/jiu648 (2015).
- 21 Noad, R. & Roy, P. Virus-like particles as immunogens. *Trends Microbiol* **11**, 438-444 (2003).
- 22 Khan, K. H. DNA vaccines: roles against diseases. *Germs* **3**, 26-35, doi:10.11599/germs.2013.1034 (2013).
- 23 Ferraro, B. *et al.* Clinical applications of DNA vaccines: current progress. *Clin Infect Dis* **53**, 296-302, doi:10.1093/cid/cir334 (2011).
- 24 Steinmetz, N. F. Viral nanoparticles in drug delivery and imaging. *Mol Pharm* **10**, 1-2, doi:10.1021/mp300658j (2013).
- 25 Ag, D. *et al.* Biofunctional quantum dots as fluorescence probe for cell-specific targeting. *Colloids Surf B Biointerfaces* **114**, 96-103, doi:10.1016/j.colsurfb.2013.09.033 (2014).
- 26 Yiyun Cheng, Z. X., Minglu Ma, Tongwen Xu. Dendrimers as Drug Carriers: Applications in Different Routes of Drug Administration. *Journal of Pharmaceutical Sciences* **97**, 123-143 (2008).
- 27 Sercombe, L. *et al.* Advances and Challenges of Liposome Assisted Drug Delivery. *Front Pharmacol* **6**, 286, doi:10.3389/fphar.2015.00286 (2015).
- 28 Zheng, D. *et al.* Influenza H7N9 LAH-HBc virus-like particle vaccine with adjuvant protects mice against homologous and heterologous influenza viruses. *Vaccine* **34**, 6464-6471, doi:10.1016/j.vaccine.2016.11.026 (2016).
- 29 Ren, Z. *et al.* H5N1 influenza virus-like particle vaccine protects mice from heterologous virus challenge better than whole inactivated virus. *Virus Res* **200**, 9-18, doi:10.1016/j.virusres.2015.01.007 (2015).
- 30 Schwartzman, L. M. *et al.* An Intranasal Virus-Like Particle Vaccine Broadly Protects Mice from Multiple Subtypes of Influenza A Virus. *MBio* **6**, e01044, doi:10.1128/mBio.01044-15 (2015).
- 31 Shen, C. *et al.* Virus-like particle-based vaccine against coxsackievirus A6 protects mice against lethal infections. *Vaccine* **34**, 4025-4031, doi:10.1016/j.vaccine.2016.06.028 (2016).
- 32 Lu, Y., Chan, W., Ko, B. Y., VanLang, C. C. & Swartz, J. R. Assessing sequence plasticity of a virus-like nanoparticle by evolution toward a versatile scaffold for vaccines and drug delivery. *Proc Natl Acad Sci U S A* **112**, 12360-12365, doi:10.1073/pnas.1510533112 (2015).
- 33 Mohsen, M. O., Zha, L., Cabral-Miranda, G. & Bachmann, M. F. Major findings and recent advances in virus-like particle (VLP)-based vaccines. *Semin Immunol* **34**, 123-132, doi:10.1016/j.smim.2017.08.014 (2017).
- 34 Jeong, H. & Seong, B. L. Exploiting virus-like particles as innovative vaccines against emerging viral infections. *J Microbiol* **55**, 220-230, doi:10.1007/s12275-017-7058-3 (2017).
- 35 Huang, R. K., Steinmetz, N. F., Fu, C. Y., Manchester, M. & Johnson, J. E. Transferrin-mediated targeting of bacteriophage HK97 nanoparticles into tumor cells. *Nanomedicine (Lond)* **6**, 55-68, doi:10.2217/nnm.10.99 (2011).

- 36 Huang, R. K. *et al.* The Prohead-I structure of bacteriophage HK97: implications for scaffold-mediated control of particle assembly and maturation. *J Mol Biol* **408**, 541-554, doi:10.1016/j.jmb.2011.01.016 (2011).
- 37 Hendrix, R. W. & Johnson, J. E. Bacteriophage HK97 capsid assembly and maturation. *Adv Exp Med Biol* **726**, 351-363, doi:10.1007/978-1-4614-0980-9_15 (2012).
- 38 Duda, R. L. Protein chainmail: catenated protein in viral capsids. *Cell* **94**, 55-60 (1998).
- 39 Kim, M. K., Jernigan, R. L. & Chirikjian, G. S. An elastic network model of HK97 capsid maturation. *J Struct Biol* **143**, 107-117, doi:10.1016/S1047-8477(03)00126-6 (2003).
- 40 Suhanovsky, M. M. & Teschke, C. M. Nature's favorite building block: Deciphering folding and capsid assembly of proteins with the HK97-fold. *Virology* **479**, 487-497, doi:10.1016/j.virol.2015.02.055 (2015).
- 41 Dhillon, E. K., Dhillon, T. S., Lai, A. N. & Linn, S. Host range, immunity and antigenic properties of lambdoid coliphage HK97. *J Gen Virol* **50**, 217-220, doi:10.1099/0022-1317-50-1-217 (1980).
- 42 Duda, R. L. *et al.* Structural transitions during bacteriophage HK97 head assembly. *J Mol Biol* **247**, 618-635, doi:10.1006/jmbi.1995.0168 (1995).
- 43 Ross, P. D. *et al.* Crosslinking renders bacteriophage HK97 capsid maturation irreversible and effects an essential stabilization. *EMBO J* **24**, 1352-1363, doi:10.1038/sj.emboj.7600613 (2005).
- 44 Nehoff, H., Parayath, N. N., Domanovitch, L., Taurin, S. & Greish, K. Nanomedicine for drug targeting: strategies beyond the enhanced permeability and retention effect. *Int J Nanomedicine* **9**, 2539-2555, doi:10.2147/IJN.S47129 (2014).
- 45 Prabhakar, U. *et al.* Challenges and key considerations of the enhanced permeability and retention effect for nanomedicine drug delivery in oncology. *Cancer Res* **73**, 2412-2417, doi:10.1158/0008-5472.CAN-12-4561 (2013).
- 46 Wyatt, C., Bartoszek, E. M. & Yaksi, E. Methods for studying the zebrafish brain: past, present and future. *Eur J Neurosci* **42**, 1746-1763, doi:10.1111/ejn.12932 (2015).
- 47 Myers, P. Z., Eisen, J. S. & Westerfield, M. Development and axonal outgrowth of identified motoneurons in the zebrafish. *J Neurosci* **6**, 2278-2289 (1986).
- 48 Westerfield, M. & Eisen, J. S. Neuromuscular specificity: pathfinding by identified motor growth cones in a vertebrate embryo. *Trends Neurosci* **11**, 18-22 (1988).
- 49 Hill, M. A. Embryology Zebrafish Development. *UNSW Embryology* (2019).
- 50 McGrath, P. Zebrafish: Methods for Assessing Drug Safety and Toxicity. **1st Edition** (2012).
- 51 Howe, K. *et al.* The zebrafish reference genome sequence and its relationship to the human genome. *Nature* **496**, 498-503, doi:10.1038/nature12111 (2013).
- 52 Kovriznykh, J. A. *et al.* Acute toxicity of 31 different nanoparticles to zebrafish (*Danio rerio*) tested in adulthood and in early life stages - comparative study. *Interdiscip Toxicol* **6**, 67-73, doi:10.2478/intox-2013-0012 (2013).
- 53 Vaughan M, v. E. R. The use of the zebrafish (*Danio rerio*) embryo for the acute toxicity testing of surfactants, as a possible alternative to the acute fish test. *. Altern Lab Anim.* **3** (2010).

- 54 Ducharme, N. A., Reif, D. M., Gustafsson, J. A. & Bondesson, M. Comparison of toxicity values across zebrafish early life stages and mammalian studies: Implications for chemical testing. *Reprod Toxicol* **55**, 3-10, doi:10.1016/j.reprotox.2014.09.005 (2015).
- 55 Staff, M. C. *Cancer Survivors: Late effects of Cancer Treatment*, (2018).
- 56 Staff, M. C. *Chemotherapy*, (2017).
- 57 Ognjanovic, S., Linabery, A. M., Charbonneau, B. & Ross, J. A. Trends in childhood rhabdomyosarcoma incidence and survival in the United States, 1975-2005. *Cancer* **115**, 4218-4226, doi:10.1002/cncr.24465 (2009).
- 58 Dasgupta, R., Fuchs, J. & Rodeberg, D. Rhabdomyosarcoma. *Semin Pediatr Surg* **25**, 276-283, doi:10.1053/j.sempedsurg.2016.09.011 (2016).
- 59 Chen, E. Y. & Langenau, D. M. Zebrafish models of rhabdomyosarcoma. *Methods Cell Biol* **105**, 383-402, doi:10.1016/B978-0-12-381320-6.00016-3 (2011).
- 60 Hobbs, G. A., Der, C. J. & Rossman, K. L. RAS isoforms and mutations in cancer at a glance. *J Cell Sci* **129**, 1287-1292, doi:10.1242/jcs.182873 (2016).
- 61 McCain, J. The MAPK (ERK) Pathway: Investigational Combinations for the Treatment Of BRAF-Mutated Metastatic Melanoma. *P T* **38**, 96-108 (2013).
- 62 Prior, I. A., Lewis, P. D. & Mattos, C. A comprehensive survey of Ras mutations in cancer. *Cancer Res* **72**, 2457-2467, doi:10.1158/0008-5472.CAN-11-2612 (2012).
- 63 Langenau, D. M. *et al.* Effects of RAS on the genesis of embryonal rhabdomyosarcoma. *Genes Dev* **21**, 1382-1395, doi:10.1101/gad.1545007 (2007).
- 64 Society, A. C. *Treating Rhabdomyosarcoma*, (2018).
- 65 Alnaim, L. Therapeutic drug monitoring of cancer chemotherapy. *J Oncol Pharm Pract* **13**, 207-221, doi:10.1177/1078155207081133 (2007).
- 66 Paci, A. *et al.* Review of therapeutic drug monitoring of anticancer drugs part 1-- cytotoxics. *Eur J Cancer* **50**, 2010-2019, doi:10.1016/j.ejca.2014.04.014 (2014).
- 67 Cabodi, S. *et al.* Integrins and signal transduction. *Adv Exp Med Biol* **674**, 43-54 (2010).
- 68 Hamidi, H., Pietila, M. & Ivaska, J. The complexity of integrins in cancer and new scopes for therapeutic targeting. *Br J Cancer* **115**, 1017-1023, doi:10.1038/bjc.2016.312 (2016).
- 69 Desgrosellier, J. S. & Cheresh, D. A. Integrins in cancer: biological implications and therapeutic opportunities. *Nat Rev Cancer* **10**, 9-22, doi:10.1038/nrc2748 (2010).
- 70 Nieberler, M. *et al.* Exploring the Role of RGD-Recognizing Integrins in Cancer. *Cancers (Basel)* **9**, doi:10.3390/cancers9090116 (2017).
- 71 Bianconi, D., Unseld, M. & Prager, G. W. Integrins in the Spotlight of Cancer. *Int J Mol Sci* **17**, doi:10.3390/ijms17122037 (2016).
- 72 Barth, T., Moller, P. & Mechttersheimer, G. Differential expression of beta 1, beta 3 and beta 4 integrins in sarcomas of the small, round, blue cell category. *Virchows Arch* **426**, 19-25 (1995).
- 73 Greish, K. Enhanced permeability and retention (EPR) effect for anticancer nanomedicine drug targeting. *Methods Mol Biol* **624**, 25-37, doi:10.1007/978-1-60761-609-2_3 (2010).
- 74 Nakamura, Y., Mochida, A., Choyke, P. L. & Kobayashi, H. Nanodrug Delivery: Is the Enhanced Permeability and Retention Effect Sufficient for Curing Cancer? *Bioconj Chem* **27**, 2225-2238, doi:10.1021/acs.bioconjchem.6b00437 (2016).

- 75 Westerfield, M. *The Zebrafish Book: A Guide for the Laboratory Use of Zebrafish (Danio rerio)*. **5th Edition** (2007).
- 76 Biolabs, N. E. *Xh01 Data Sheet* (2018).
- 77 Scientific, T. F. T042-Technical Bulletin NanoDrop Spectrophotometers 260/280 and 260/230 Ratios (2009).
- 78 Howe, D. G. *et al.* ZFIN, the Zebrafish Model Organism Database: increased support for mutants and transgenics. *Nucleic Acids Res* **41**, D854-860, doi:10.1093/nar/gks938 (2013).
- 79 Schneider, C. A., Rasband, W. S. & Eliceiri, K. W. NIH Image to ImageJ: 25 years of image analysis. *Nat Methods* **9**, 671-675 (2012).
- 80 Microsoft Excel for Mac v. 16.20 (181208) (2018).
- 81 GNU Image Manipulation Program 2.10.4 (2018).
- 82 Graph Pad Prism for Windows v. 7.00 (Graph Pad Software, La Jolla, CA, 2018).
- 83 Singh, P. *et al.* Bio-distribution, toxicity and pathology of cowpea mosaic virus nanoparticles in vivo. *J Control Release* **120**, 41-50, doi:10.1016/j.jconrel.2007.04.003 (2007).
- 84 Hachicho, N. *et al.* Body Mass Parameters, Lipid Profiles and Protein Contents of Zebrafish Embryos and Effects of 2,4-Dinitrophenol Exposure. *PLoS One* **10**, e0134755, doi:10.1371/journal.pone.0134755 (2015).
- 85 Tolomelli, A., Galletti, P., Baiula, M. & Giacomini, D. Can Integrin Agonists Have Cards to Play against Cancer? A Literature Survey of Small Molecules Integrin Activators. *Cancers (Basel)* **9**, doi:10.3390/cancers9070078 (2017).
- 86 Wang, X., Li, L. & Liu, D. Expression analysis of integrin beta1 isoforms during zebrafish embryonic development. *Gene Expr Patterns* **16**, 86-92, doi:10.1016/j.gep.2014.10.001 (2014).
- 87 Ruoslahti, E. RGD and other recognition sequences for integrins. *Annu Rev Cell Dev Biol* **12**, 697-715, doi:10.1146/annurev.cellbio.12.1.697 (1996).
- 88 Kapp, T. G. *et al.* A Comprehensive Evaluation of the Activity and Selectivity Profile of Ligands for RGD-binding Integrins. *Sci Rep* **7**, 39805, doi:10.1038/srep39805 (2017).